Environmental Science & Technology

Article

pubs.acs.org/est

Hydrous Mineral Dehydration Around Heat-Generating Nuclear Waste in Bedded Salt Formations

Amy B. Jordan,*[,†] Hakim Boukhalfa,[‡] Florie A. Caporuscio,[‡] Bruce A. Robinson,[§] and Philip H. Stauffer[†]

[†]EES-16: Computational Earth Science, MS T003, Los Alamos National Laboratory, Los Alamos, New Mexico 87545, United States
[‡]EES-14: Earth System Observations, MS J-599, Los Alamos National Laboratory, Los Alamos, New Mexico 87545, United States
[§]SPO-CNP: Civilian Nuclear Programs, MS H816, Los Alamos National Laboratory, Los Alamos, New Mexico 87545, United States

Supporting Information

ABSTRACT: Heat-generating nuclear waste disposal in bedded salt during the first two years after waste emplacement is explored using numerical simulations tied to experiments of hydrous mineral dehydration. Heating impure salt samples to temperatures of 265 °C can release over 20% by mass of hydrous minerals as water. Three steps in a series of dehydration reactions are measured (65, 110, and 265 °C), and water loss associated with each step is averaged from experimental data into a water source model. Simulations using this dehydration model are used to predict temperature, moisture, and porosity after heating by 750-W waste canisters, assuming hydrous mineral mass fractions from 0 to 10%. The formation of a three-phase heat pipe (with counter-circulation of vapor and brine) occurs as water vapor is driven away from the heat source, condenses, and flows back toward the heat source, leading to changes in porosity, permeability, temperature, saturation, and thermal conductivity of the backfill salt surrounding the waste canisters. Heat pipe formation depends on temperature, moisture availability, and mobility. In certain cases, dehydration of hydrous minerals provides sufficient extra moisture to push the system into a sustained heat pipe, where simulations neglecting this process do not.

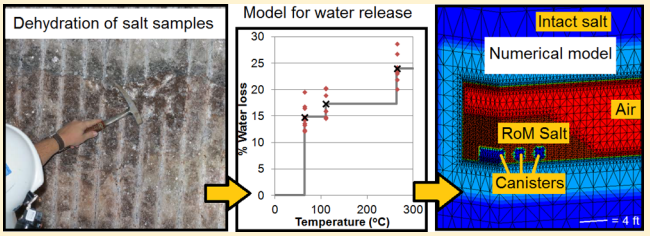

INTRODUCTION

The question of where to store the nation's heat-generating nuclear waste (HGNW) provides motivation for scientific research on disposal options. HGNW is composed of both high-level nuclear waste (HLW) from nuclear weapons production and spent nuclear fuel (SNF) from civilian and defense reactors. A number of potential geologic media have been proposed for HGNW repositories, including volcanic tuff, shale, clay, crystalline rock, and both bedded and domal salt.[1−3]

Multiple geologically stable salt formations in the U.S. may be suitable for nuclear waste disposal.[1] Salt has unique temperature-dependent viscoplastic properties that contribute to self-sealing of tunnels and other disturbed zones to low permeabilities associated with intact salt[4] in relatively short time periods (tens to hundreds of years);[1,5] it also has a high thermal conductivity when intact or reconsolidated; and salt is relatively easy to mine. These characteristics make salt a favorable option for locating a nuclear waste repository.[1] Long-term performance of a potential HGNW repository in salt will be dominated by the mechanical deformation of salt surrounding the waste, which will ultimately lead to room closure of the drifts and isolation of the waste canisters in low-permeability intact salt, but physical and chemical processes functioning around the HGNW in the first few years have implications for extended repository evolution.[1,6]

Domal salt formations are being extensively studied for nuclear waste storage in Germany[7,8] and in the United States for HGNW and natural gas storage.[7,9] Bedded salt has been studied at the Waste Isolation Pilot Plant (WIPP) in southern New Mexico, and elsewhere in the U.S.[7] Recently, a new "in-drift" waste emplacement strategy for disposal of HGNW has been proposed.[10] In this method, waste canisters are placed directly on the floor of horizontal drifts, and run-of-mine (RoM) excavated material is used as backfill over them (Figure 1). In the configuration used for this study, RoM salt fills the drift to the back, to both sides, and leaves an air gap between the top of the backfill and the roof of the drift. Bedded salt is far more heterogeneous and contains a higher mass fraction of hydrous minerals, such as clay and gypsum, than domal salt.[11] Thus, in-drift disposal in bedded salt will result in hydrous minerals being incorporated into the RoM salt backfill.

Clays in bedded salt may be present both in relatively pure layers up to several cm thick, or finely dispersed.[4,12] The temperature, timing, and amount of water released from clay dehydration depends on the presence of electrolytes, relative humidity, temperature, and pressure.[13] Sulfate minerals are also identified in WIPP samples, such as gypsum ($CaSO_4{\cdot}2H_2O$), anhydrite ($CaSO_4$), and polyhalite ($K_2Ca_2Mg(SO_4)_4{\cdot}2H_2O$). Gypsum (21 wt % water) can transition directly to anhydrite or

Received: February 25, 2015
Revised: May 9, 2015
Accepted: May 12, 2015
Published: May 12, 2015

DOI: 10.1021/acs.est.5b01002
Environ. Sci. Technol. 2015, 49, 6783−6790

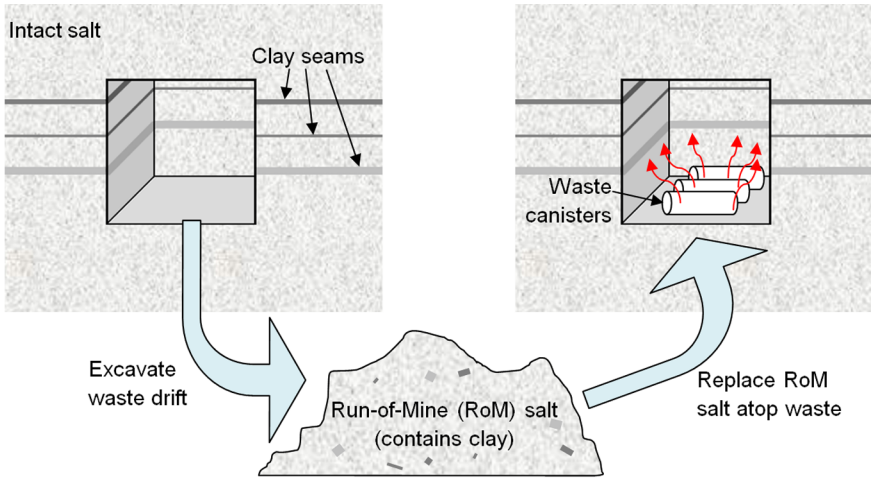

Figure 1. Schematic of the in-drift waste disposal concept.

to metastable bassanite ($CaSO_4{\cdot}0.5H_2O$), followed by a bassanite to anhydrite transition. Other hydrous minerals that may be present include carnallite ($KMgCl_3{\cdot}6H_2O$), kieserite ($MgSO_4{\cdot}H_2O$), and bischofite ($MgCl_2{\cdot}6H_2O$).[14] Temperatures for dehydration transitions have been measured for several scenarios by previous authors, with varying results.[13−16]

Heating at the base of a high-permeability pile of RoM salt leads to natural convection and the creation of a chimney with hot air rising above the waste packages. If there is sufficient mobile water and heat supplied by the waste, a three-phase heat pipe may form in the RoM salt. In a heat pipe, liquid water is vaporized in a boiling region, convects and diffuses along vapor concentration gradients to cooler regions where it recondenses and flows back toward the heat source by a combination of gravity flow and capillary pressure gradients.[17,18] If brine re-enters the boiling region, it will vaporize and deposit dissolved salt as a precipitate, contributing to the buildup of a low-porosity rind around the waste.

Bench-scale laboratory investigations have produced heat pipes in moist salt under relevant repository conditions.[19] One component of the heat pipe process has been observed in situ at WIPP: deposition of low-porosity salt during boiling of brine.[20] Numerical simulations of in-drift disposal of HGNW show that if a heat pipe forms, the process can cause significant changes in the time evolution of temperature, saturation, and porosity of the backfilled RoM salt around the waste in the first few years after waste disposal.[21]

Numerical modeling of HGNW disposal in salt has been performed by multiple groups for WIPP and for other salt repositories worldwide,[7] but simulation of the strongly coupled thermal, hydrological, mechanical, and chemical (THMC) processes have been done only at small spatial scales.[22] Current state-of-the-art simulators for repository-scale simulations have been limited to incomplete coupling, e.g., only simultaneous coupling of THM processes to capture the viscoplastic reconsolidation behavior of salt, or only coupled THC processes to include the effects of porosity change from precipitation and dissolution across temperature gradients.[21,23−26] The THC model developed here does not include mechanical effects that lead to room closure and RoM reconsolidation. However, the modeled THC processes operating on short time scales may be important to the salt repository safety case because of impacts including different rates of reconsolidation of RoM backfill based on moisture content,[5,27] altered potential for corrosion of the waste canisters, gas generation, and a modified thermal regime (e.g., maximum temperatures reached) immediately surrounding the waste.

Initial coupled THC simulations indicated that the amount and mobility of water in the RoM backfill would play an important role in governing whether an active heat pipe would form.[21] Considerable uncertainty exists in the amount, production, and retention characteristics of water in bedded salt formations.[14] Water in the system is found as fluid inclusions in salt crystals, within the boundaries between salt grains, or associated with hydrous minerals. The mobility of these different populations of water, their chemical composition, and their relative amounts vary significantly within bedded salt. Among these different water populations, water associated with hydrous minerals may represent a substantial fraction of moisture contained in salt.[15] This paper presents a synthesis of ongoing model development research[21] related to the impact of water-producing physicochemical processes caused by the heating of hydrous minerals. Our research advances prior HGNW models for bedded salt and presents an example that shows the potential importance of including mineral dehydration in salt repository calculations.

The goal of this study is to incorporate a new empirically derived hydrous mineral dehydration model for bedded salt into a state-of-the-art coupled numerical simulator to predict the impact of available moisture on fluid and heat transport. In the following sections, we first present recent experimental hydrous mineral dehydration data from bedded salt samples. Next, these data are used to develop a simple model for hydrous mineral water releases as a function of temperature. This model is then implemented into a numerical porous flow simulator. Simulations are run for 2 years of heating by HGNW canisters emplaced using the in-drift disposal method. Because of large uncertainties in flow properties, hydrous mineral mass fraction, and initial water content of RoM salt, many simulations were performed across parameter space. We present a subset of these simulations that highlights the importance of including the hydrous mineral water source.

MATERIALS AND METHODS

Salt Sampling and Characterization. Thirteen RoM salt samples (100−200 g) were collected from WIPP, which is mined in a bedded Permian-age salt formation 650 m below the

DOI: 10.1021/acs.est.5b01002
Environ. Sci. Technol. 2015, 49, 6783−6790

surface, that represented a range of impurity content and mass fractions in the salt, including mapped units such as clay seam F, the orange marker bed, and relatively pure halite from the drift floor in a freshly excavated room.[4,15] The samples were sealed in plastic bags using an impulse heater immediately after exiting the underground mine, and were kept in a sealed, large plastic container until utilized. Residual minerals from the samples were analyzed by X-ray diffraction (XRD). Residues from clay seam F and orange marker bed samples were composed primarily of corrensite—$(Mg,Fe,Al)_9((Si,Al)_8O_{20})(OH)_{10}\cdot 4H_2O$—with minor amounts of quartz, magnesite, mica, kaolinite (or possibly chlorite), hematite, and anhydrite. All samples contained halite.

Gravimetric Characterization of Salt Dehydration. The bulk samples (100−200 g) were weighed at the start of the experiment, heated to certain designated temperatures, and weighed again every 8−12 h until the weight stabilized (typically, within 24−72 h). Once a constant weight was achieved at the first temperature, the sample was heated to the next desired temperature and the process was repeated. The temperatures were 65, 110, 165, and 265 °C. These temperatures were chosen based on expected dehydration reactions. A portion of the samples were removed from the heaters after 65 and 110 °C and allowed to rehydrate. The maximum vacuum applied was 15 mmHg at 265 °C to ensure the release of all water associated with the rock salt. The moisture released from these experiments was not collected.

Thermogravimetric Analysis of Salt and Accessory Minerals. Thermogravimetric analyses (TGA) of natural clay-rich samples and washed clay samples were obtained using a TA Instrument Inc. Q500 coupled with a mass spectrometer that allows resolution of ion masses ±1.0 amu. The instrument was operated by equilibrating the samples at room temperature for 2.0 min followed by a constant temperature ramp of 5 °C/min from room temperature to 350 °C. The instrument was operated under a constant 40 mL/min flow of high-purity nitrogen. All experiments were performed on clay specimens of 1.5−2.0 mg collected from WIPP salt samples obtained from clay seam F. A fraction of the gas flow through the sample was continuously run through the mass spectrometer, allowing characterization of the ion masses of the substances released from the sample as a function of temperature.

Numerical Model. The porous media flow and transport simulator FEHM was used to explore the impacts of mineral dehydration on mass transfer for an in-drift repository-scale example. FEHM uses the control volume finite element method to solve the governing equations of mass and momentum conservation, assuming a multiphase form of Darcy's Law is valid for all phases across the domain, and includes advection, diffusion, and phase changes.[28] Many new capabilities have been added to FEHM to model the tightly coupled THC processes of fluid transport in heated salt in the RoM backfill and DRZ, including the following:[21] porosity change from precipitation/dissolution of salt; salt solubility increasing with temperature; permeability increasing with porosity using a power law model with experimentally derived coefficients;[29] thermal conductivity of salt as an empirical function of porosity and temperature;[25] vapor pressure of water as an empirical function of concentration and temperature;[30] and water vapor diffusion as a function of saturation, porosity, pressure, and temperature. The Millington−Quirk approach[31] is used to calculate the tortuosity (τ), which modifies vapor-phase free-air diffusivity based on air saturation (S_a) and porosity (φ), by

$$\tau = (S_a\varphi)^{7/3}/\varphi^2 \quad (1)$$

A hydrous mineral dehydration model based on our experimental results was developed and used in numerical simulations of a drift in a HGNW repository. Five heated waste canisters, each a fixed enthalpy source of 750 W, 0.3-m radius, and 2.4-m length, were spaced 0.3 m apart on the floor of a 4.9 m wide by 3.0 m high drift. Salt backfill over the canisters extended 1.8 m in height above the drift floor, to the sides of the drift (4.9 m), and 8.5 m in length at the bottom, tapering toward the top (total volume of RoM salt: 57 m^3). A section of the numerical mesh developed for simulations of this experiment is shown in Figure 2. The model represents a

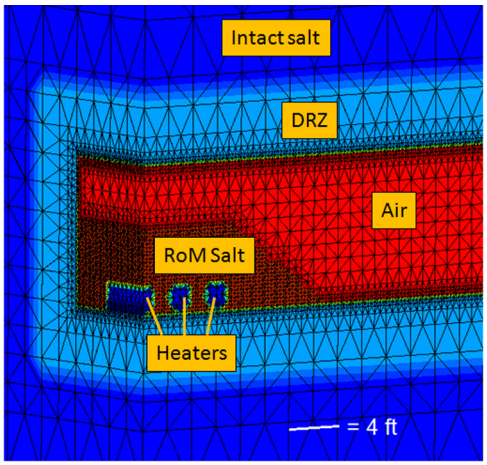

Figure 2. Numerical mesh showing the zones of the model: intact salt, damaged rock zone (DRZ), air, run-of-mine (RoM) backfill, and the heated waste canisters.

quarter space, with reflection boundaries on both faces seen in Figure 2. The zones represent the undisturbed, intact salt of the repository; the damaged rock zone (DRZ) with enhanced permeability due to damage related to excavating the drift; air; the RoM salt backfill; and the heated waste canisters.

The DRZ permeability was initially 10^{-19} m^2, while the intact salt permeability was 10^{-21} m^2. This model, which was used for short-term calculations, does not include any mechanical deformation of salt. Following excavation of the drifts, the permeability of the DRZ is expected to evolve anisotropically due to fracture healing and viscoplastic creep that eventually leads to room closure;[4] in the current work, permeability change in the DRZ is only caused by salt precipitation and dissolution. RoM backfill reconsolidation may affect the porosity structure and have important feedbacks on hydrological parameters, as investigated by multiple experiments and TM and THM models.[5,23,24,32]

The RoM backfill was modeled to contain accessory hydrous minerals. The typical accessory mineral content (f_c) in bedded salt formations is highly variable, ranging from very little (<1 wt % for nearly pure halite)[1] to argillaceous halite (up to 5 wt %),[12] with even higher amounts (up to 16 wt % in our samples) found in the thin clay seams and marker beds.[12,14,15]

The simulations are performed in volumetric saturation space, with initial volumetric saturations (S_i) varying from 0.01 to 0.07 (1−7%), while the experimental data are presented in water mass fraction units (mass of water/mass of sample). At a porosity of 0.35 and salt density of 2165 kg/m^3, volumetric saturation of 1% corresponds to mass fraction of 0.25 wt %, and

DOI: 10.1021/acs.est.5b01002
Environ. Sci. Technol. 2015, 49, 6783−6790

7% volumetric saturation is 1.8 wt %. Maximum capillary suction ($P_{c,max}$) at residual saturation and S_i are highly uncertain and are varied in our simulations. The parameters used in the simulations discussed in the main text and Supporting Information (SI) are shown in Table 1. Values of $P_{c,max}$ greater

Table 1. Simulation Parameters

		f_c (%)	S_i (%)	$P_{c,max}$ (MPa)
case 1	(a)	0	1	0.2
	(b)	10	1	0.2
case 2	(a)	0	7	1.0
	(b)	10	7	1.0
case 3	(a)	10	1	0.2
	(b)	10	1	1.0
case 4 (SI)	(a)	0	5	0.2
	(b)	0	10	0.2
	(c)	0	10	1.0

than those observed[29] are included because of uncertainty in the grain size distribution in RoM salt as well as extrapolation to very low saturation (e.g., in the boiling front very near the canisters). An inverse linear relationship between capillary suction and saturation was used due to large uncertainties in the retention characteristics of mixed-grain size, consolidating RoM salt under conditions of changing porosity.[21,29]

RESULTS AND DISCUSSION

Moisture Release from Run-of-Mine Salt as a Function of Temperature. In the dehydration experiment, an initial weight gain ranging from 0.1−0.8 wt % occurred for all samples, which was due to moisture absorption during equilibration of samples at room temperature before the start of the dehydration experiment. Heating clay-rich salt samples to 65 °C resulted in total sample weight loss of 1.2−2.1 wt %. By fraction of clay and other accessory minerals, the loss was 12.1−19.6% of hydrous mineral mass (average 14.8%) at 65 °C. Clear salt samples, which contained very small amounts of accessory minerals, lost less than 0.25 wt % of their total weight at 65 °C. Dehydration of the clay rich samples at 65 °C was reversible; 3 samples removed from the oven and placed in a moist chamber recovered their weight and then continued to accumulate water rapidly.

The clay-rich samples heated to 110 °C lost 1.3−2.5 wt %. By hydrous mineral fraction this was 14.6−20.4% of clay mass, with an average of 17.3% (or 2.5% additional mass loss from dehydration following the water loss at 65 °C). Clear salt with minimal accessory minerals had water loss of less than 0.06 wt %.

At 165 °C, the samples lost no additional weight after heating for 15 h. The dehydration process was still reversible; a subset of samples removed from the experiment to a moist environment rapidly recovered all the moisture lost and then accumulated additional moisture due to the abundance of clay in the samples, which can undergo rapid and reversible hydration/dehydration processes, and water sorption onto the surface of both the clay and RoM salt grains.

The temperature was raised to 265 °C for the final test of water loss. Samples lost a total of 0.09−3.5 wt %, or 20.1−28.7% of hydrous mineral mass (average of 24.0%, or 6.7% more following the previous dehydration to 110 °C).

The total weight loss is correlated with samples' accessory minerals content, rejecting the hypothesis that the water released upon heating is primarily intergranular pore fluid or intragranular brine inclusions for the clay-rich samples. Furthermore, the reversible water loss for T < 110 °C is consistent with temperatures under which corrensite undergoes hydration/dehydration processes: the XRD and TGA results provide strong evidence of loss of interlayer water (5−13 wt %) at 65−75 °C.[15] Concurrently, at around 75 °C, the gypsum to bassanite phase transformation can release up to 15 wt % water. The cause of the water loss at higher temperatures may be from further dehydration of both mineral groups, particularly bassanite to anhydrite, which can release an additional 6 wt % water.

TGA experimental and mass spectrometer data are shown in Figure 3, showing the weight loss and heat flow recorded

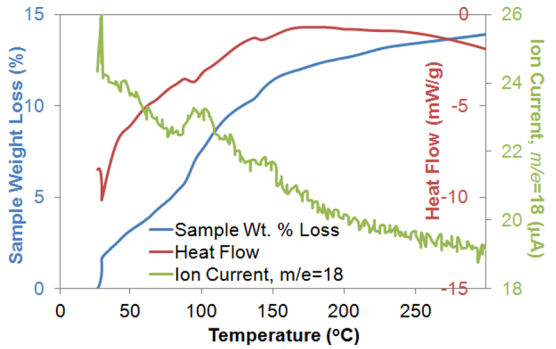

Figure 3. Dehydration of accessory minerals from a sample obtained from clay seam F at WIPP. The blue line shows the weight loss as a function of temperature, the red line indicates the heat flow during dehydration, and the green line indicates the ion current for m/e = 18.

during the dehydration of a clay-rich sample, along with the ion current for mass to charge ratio (m/e) of 18 (water). The data show an increase in the ion current indicating an initial water release, additional water release just below 50 °C and slightly above 50 °C, between 90 and 100 °C, and between 140 and 170 °C. The weight loss and energy flow curves show significant changes in the same temperature domains, with decreases in heat flow during mass loss indicating endothermic processes. Similar experiments performed on clay samples that have been washed repeatedly to eliminate any soluble minerals show a more pronounced weight loss between 50 and 70 °C and lose the features visible between 90 and 100 °C and between 140 and 170 °C (SI Figure S1). The weight loss observed at 50 °C is most likely from water absorbed to mineral grain surfaces, primarily clays. The second weight loss (70 °C) is coincident with dehydration experiments of corrensite clay from previous experiments,[15] along with the transition of gypsum to bassanite. The third weight loss, occurring near 100 °C, is most likely due to initial phase transformation of bassanite to anhydrite.[33] The water loss at 150 °C may also be due to the bassanite to anhydrite phase transformation, which is kinetically driven and may occur in stages. Alternatively, the water loss at 150 °C may be due to another mineral breakdown (such as $MgCl_2$) which undergoes several dehydration stages, one of which occurs between 140 and 170 °C. Polyhalite loses its hydrate water at temperatures above 250 °C, and can lose up to 6 wt % as water. Carnallite, kieserite, and bischofite may also contribute to water loss of RoM samples under heating.[15] Above 250 °C, water loss may be contributed from intragranular fluid inclusion release due to decrepitation.[34] Although the measured weight loss curves are highly useful for

DOI: 10.1021/acs.est.5b01002
Environ. Sci. Technol. 2015, 49, 6783−6790

developing a water source term model, additional experimental characterization of the clay composition and the dehydration of the different species is needed to confirm the processes producing the temperature-dependent weight loss curves.

Numerical Dehydration Model. Averages of the water loss data as a function of temperature from the bulk salt samples were used to develop a hydrous mineral dehydration water release model (Figure 4).[21] The model uses a simple

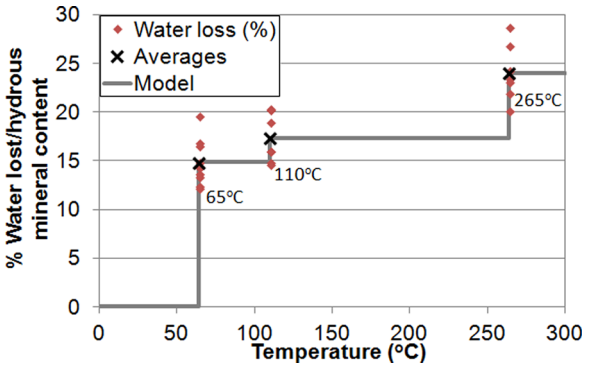

Figure 4. Weight lost as a percentage of hydrous mineral weight during the heating experiment and the stepwise dehydration model.[21]

stair-step function, and does not allow rehydration. Because temperatures monotonically increase and remain elevated in the backfill salt around the waste for the short-term (<2 years) duration of these model runs, rehydration is not expected. Representing hydrous mineral dehydration as one-time releases is a simplification of kinetically driven water release as a function of temperature, justified by uncertainty due to heterogeneity in hydrous mineral quantities and relative abundances in a repository setting, and with the caveat that this dehydration model is used only to demonstrate order-of-magnitude effects that may be of importance to the repository safety case.

As implemented in FEHM, the hydrous mineral dehydration model can be applied to selected nodes or zones within the model, and differing mass fractions of hydrous mineral content can be specified across the model, e.g., if clay seams are explicitly modeled. On the basis of the averaged experimental data discussed above, at 65 °C, 14.8% of the mass of hydrous minerals in the node is added as a source term in a one-time release. At 110 °C, an additional percentage is released as water (2.5%), and at 265 °C, more water is released (6.7%) for a total mass release of 24.0% of the hydrous mineral weight. For a given node for which the dehydration model is invoked, for a specified mineral mass fraction f_c, the mass of water produced for the first 65 °C dehydration is given by

$$M_w = f_1 f_c (1 - \varphi_i)\rho_c V_{cell} \quad (2)$$

where f_1 is the fractional weight in water released at the first dehydration (0.148), φ_i is the initial porosity of the node, ρ_c is the density of clay, and V_{cell} is the volume of the node. The water mass production for the second and third dehydration temperatures follows similarly, with f_2 = 0.025 and f_3 = 0.067 replacing f_1 in eq 2 (Figure 4). The release of pure water from mineral dehydration causes dissolution of solid salt and a corresponding change in porosity.[21] The implementation of the new hydrous mineral dehydration model in FEHM was tested in a simplified 6-node simulation and it compared closely to calculated values.[21]

Numerical Model Results. For a Case 1b, Figure 5 shows the porosity and temperature at 460 days. The initial porosity

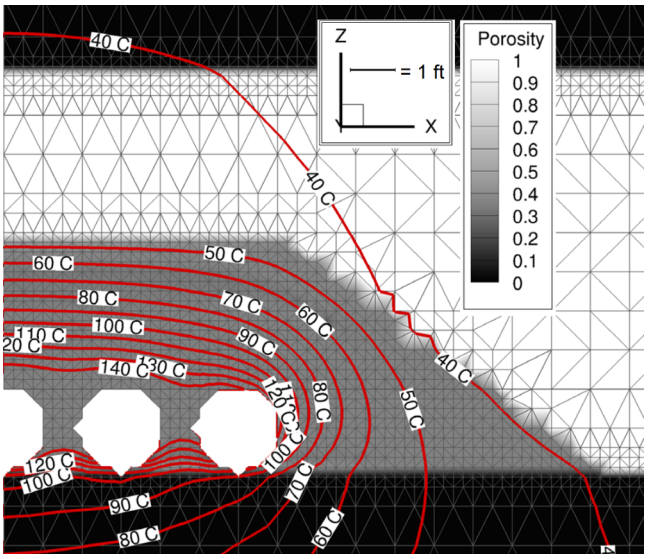

Figure 5. Porosity and temperature around the heaters at 460 days for a case with f_c = 10% in the RoM salt. RoM φ_i = 0.35, S_i = 1%, and $P_{c,max}$ = 0.2 MPa (Case 1b).

in the DRZ above and below the drift is 0.01, porosity in the air is 0.999, and initial porosity in the RoM salt pile, where significant precipitation and dissolution would be expected if a heat pipe were to form, is φ_i = 0.35. After 460 days of heating, however, the porosity is not significantly changed from the initial state, in this case. This indicates very little heat pipe activity.

The saturation, porosity, and temperature differences at 460 days between 10% clay and the corresponding simulation with no clay are shown in Figure 6. Only minor differences are observed in this example in the temperature and porosity. That is, the dehydration process has only a minor impact on the final state of the system in Case 1.

In Figure 6c, a ring of higher saturation persists outside the boiling region for the hydrous mineral-bearing case. The core of the RoM salt is also cooler because of latent heat transfer. The total amount of water produced in the simulation with 10% hydrous minerals in the RoM salt pile in the model (one-quarter of the full salt pile) is 119 kg at 460 days. By comparison, the total initial amount of water in the RoM salt with S_i = 0.01 and porosity 0.35 is 50.4 kg.

The preceding example is a case where hydrous mineral dehydration causes only small changes in the final temperature and porosities observed after 460 days of heating. Case 2 shows that the presence of hydrous minerals can cause major differences, with evidence for heat pipe activity when dehydration releases additional water (Figure 7). Evidence for heat pipe activity includes lower porosity around the heaters from evaporating brine, a high-porosity region where water vapor condenses and dissolves the RoM solids, and a flatter temperature gradient around the canisters[35] (Figure 7b). Differences in temperature and porosity at 460 days are shown in Figure 8 for simulations with and without hydrous mineral dehydration. This time, the difference in final temperature (Figure 8a) is significant, with heater temperatures up to 25 °C cooler. The heat pipe efficiently transports heat

DOI: 10.1021/acs.est.5b01002
Environ. Sci. Technol. 2015, 49, 6783−6790

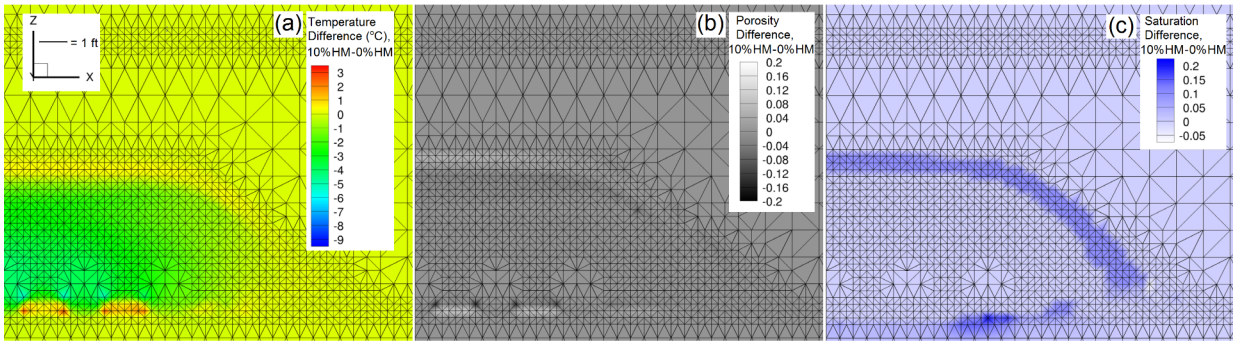

Figure 6. Differences of f_c = 10% (Case 1b) minus pure halite (f_c = 0%, Case 1a) at 460 days with S_i = 1% and $P_{c,max}$ = 0.2 MPa: (a) temperature, (b) porosity, and (c) saturation.

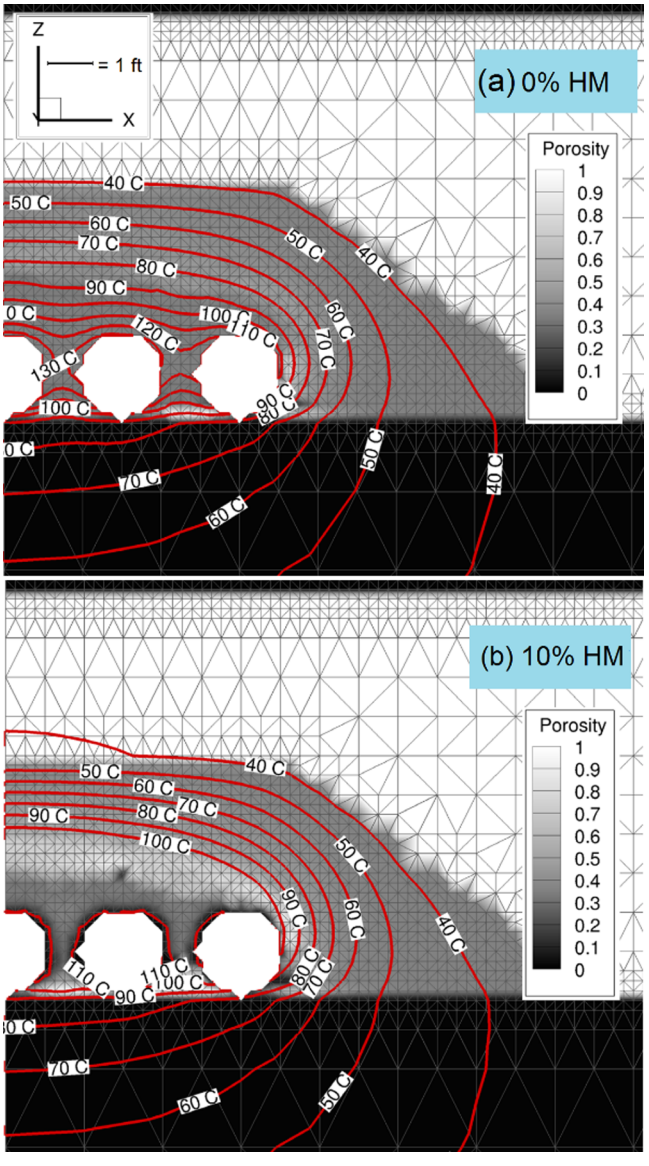

Figure 7. Porosity and temperature around the heaters at 460 days for (a) Case 2a, f_c = 0% and (b) Case 2b, f_c = 10%. RoM φ_i = 0.35, S_i = 7%, and $P_{c,max}$ = 1 MPa.

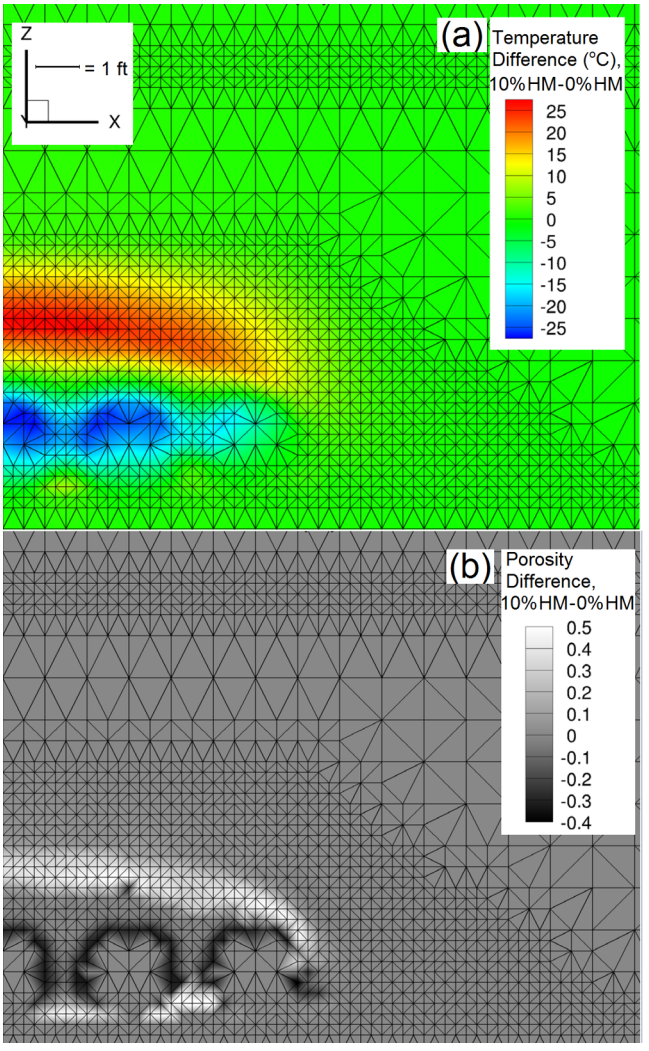

Figure 8. Differences of f_c = 10% (Case 2b) minus pure halite (f_c = 0%, Case 2a) at 460 days with S_i = 7% and $P_{c,max}$ = 1 MPa: (a) temperature and (b) porosity.

away from the waste,[17] leading to cooler maximum temperatures and less dry-out around the canisters. Beyond the condensation front, the higher saturations of the case with the hydrous mineral dehydration model leads to lower thermal diffusivity and thus hotter temperatures.

The choice of $P_{c,max}$ at zero saturation has an effect on the moisture distribution as well (case 3), as discussed in the SI (Figures S2 and S3).

Implications for Disposal of Heat-Generating Nuclear Waste. Depending on uncertain factors such as initial moisture content and retention properties of the RoM salt, the addition

DOI: 10.1021/acs.est.5b01002
Environ. Sci. Technol. 2015, 49, 6783−6790

of water from hydrous mineral dehydration may make a significant difference in final temperature, moisture, and porosity redistribution. The redistribution of mass, moisture, and temperature at early times may impact the time evolution of salt plasticity and mechanical deformation at longer time scales. Additionally, other strongly coupled thermal, hydrological, and chemical processes around heat-generating nuclear waste in bedded salt formations are modified by water released from minerals. Ongoing model development research and experimental work will improve the ability to make longer-term predictions, such as by including mechanical effects related to viscoplastic creep in the host rock and reconsolidation of the RoM salt.

■ ASSOCIATED CONTENT

Supporting Information

Additional TGA analyses and simulation results. The Supporting Information is available free of charge on the ACS Publications website at DOI: 10.1021/acs.est.5b01002.

■ AUTHOR INFORMATION

Corresponding Author

*Phone: 505-667-1049; fax: 505-665-3285; e-mail: ajordan@lanl.gov.

Notes

The authors declare no competing financial interest.

■ ACKNOWLEDGMENTS

This work was funded by the DOE Office of Nuclear Energy and Office of Environmental Management. We are grateful for reviews of drafts of this article by Mark Person, Prasad Nair, Roger Nelson, and others. Computational mesh support was provided by Carl Gable, Terry Miller, and Dylan Harp. Thanks are also due to Brian Dozier and Doug Weaver for assistance collecting samples. Finally, we thank the reviewers from this journal, whose comments led to revisions which greatly improved this paper.

■ REFERENCES

(1) Hansen, F. D.; Leigh, C. D. *Salt Disposal of Heat-Generating Nuclear Waste*; Sandia National Laboratories Report, SAND2011-0161; 2011; http://prod.sandia.gov/techlib/access-control.cgi/2011/110161.pdf.

(2) Bodvarsson, G. S.; Boyle, W.; Patterson, R.; Williams, D. Overview of scientific investigations at Yucca Mountain—the potential repository for high-level nuclear waste. *J. Contam. Hydrol.* **1999**, *38* (1), 3−24 DOI: 10.1016/S0169-7722(99)00009-1.

(3) Neuzil, C. E. Can Shale Safely Host US Nuclear Waste? *Trans. Am. Geophys. Union* **2013**, *94* (30), 261−262.

(4) Beauheim, R. L.; Roberts, R. M. Hydrology and hydraulic properties of a bedded evaporite formation. *J. Hydrol.* **2002**, *259* (1), 66−88 DOI: 10.1016/S0022-1694(01)00586-8.

(5) Hansen, F. D.; Popp, T.; Wieczorek, K.; Stuhrenberg, D. *Granular Salt Summary: Reconsolidation Principles and Applications*; Prepared for U.S. Department of Energy Used Fuel Disposition, Report FCRD-UFD-2014-000590; 2014.

(6) *The Waste Isolation Pilot Plant: A Potential Solution for the Disposal of Transuranic Waste*; National Research Council: Washington, DC, 1996; http://www.nap.edu/openbook.php?isbn=0309054915.

(7) Kuhlman, K. L.; Malama, B. *Brine Flow in Heated Geologic Salt*; Sandia National Laboratories Report, SAND2013-1944: 2013; http://prod.sandia.gov/techlib/access-control.cgi/2013/131944.pdf.

(8) Mönig, J.; Beuth, T.; Wolf, J.; Lommerzheim, A.; Mrugalla, S. Development Based on a Site-Specific Features, Events and Processes (FEP) Database-13304. In *Proceedings WM2013 Conference*, Phoenix, AZ, 2013.

(9) Istvan, J. A.; Evans, L. J.; Weber, J. H.; Devine, C. Rock mechanics for gas storage in bedded salt caverns. *Int. J. Rock Mech. Min. Sci.* **1997**, *34* (3), 142.e1−142.e12 DOI: 10.1016/S1365-1609(97)00108-1.

(10) Carter, J. T.; Rodwell, P. O; Robinson, B. A.; Kehrman, B. *Defense Waste Salt Repository Study: Fuel Cycle Research & Development*; Prepared for U.S. Department of Energy Used Fuel Disposition, Report FCRD-UFD-2012-000113; 2012.

(11) Carter, N. L.; Hansen, F. D.; Senseny, P. E. Stress magnitudes in natural rock salt. *J. Geophys. Res.: Solid Earth* **1982**, *87* (B11), 9289−9300 DOI: 10.1029/JB087iB11p09289.

(12) Stein, C. L. *Mineralogy in the Waste Isolation Pilot Plant (WIPP) Facility Stratigraphic Horizon*; Sandia National Laboratories Report, SAND-85-0321; 1985; http://www.wipp.energy.gov/library/cra/2009_cra/references/Others/Stein_1985_Mineralogy_in_the_WIPP_SAND85_0321.pdf.

(13) Freyer, D.; Voight, W. Crystallization and phase stability of $CaSO_4$ and $CaSO_4$−based salts. *Monatsh. Chem.* **2003**, *134* (5), 693−719 DOI: 10.1007/s00706-003-0590-3.

(14) Roedder, E.; Bassett, R. L. Problems in determination of the water content of rock-salt samples and its significance in nuclear-waste storage siting. *Geology* **1981**, *9* (11), 525−530 DOI: 10.1130/0091-7613(1981)9.

(15) Caporuscio, F. A.; Boukhalfa, H.; Cheshire, M. C.; Jordan, A. B; Ding, M. *Brine Migration Experimental Studies for Salt Repositories*; Los Alamos National Laboratory Document, LA-UR-13-27240; 2013; http://energy.gov/sites/prod/files/2013/12/f5/BrineMigrationinExpermntsSaltR1.pdf.

(16) Shcherban, J. P.; Shirokikh, I. N. Thermodynamic and experimental data on stability of gypsum, hennihydrate, and anhydrite under hydrothermal conditions. *Int. Geol. Rev.* **1971**, *13* (11), 1671−1673 DOI: 10.1080/00206817109475625.

(17) Udell, K. S. Heat transfer in porous media considering phase change and capillarity—the heat pipe effect. *Int. J. Heat Mass Transfer* **1985**, *28* (2), 485−495.

(18) Doughty, C.; Pruess, K. A similarity solution for two-phase fluid and heat flow near high-level nuclear waste packages emplaced in porous media. *Int. J. Heat Mass Transfer* **1990**, *33* (6), 1205−1222.

(19) Olivella, S.; Castagna, S.; Alonso, E. E.; Lloret, A. Porosity variations in saline media induced by temperature gradients: experimental evidences and modelling. *Transp. Porous Media* **2011**, *90* (3), 763−777 DOI: 10.1007/s11242-011-9814-x.

(20) Krumhansl, J. L.; Stein, C. L.; Jarrell, G. D.; Kimball, K. M. *Summary of WIPP Room B Heater Test Brine and Backfill Material Data*; Sandia National Laboratories Report, SAND-90-0626; 1991.

(21) Stauffer, P. H.; Harp, D. R.; Jordan, A. B.; Lu, Z.; Kelkar, S.; Kang, Q.; Ten Cate, J.; Boukhalfa, H.; Labayed, Y.; Reimus, P. W.; Caporuscio, F. A.; Miller, T. A.; Robinson, B. A. *Coupled Model for Heat and Water Transport in a High Level Waste Repository in Salt*; Los Alamos National Laboratory Document, LA-UR-13-27584; 2013; http://www.energy.gov/sites/prod/files/2013/12/f5/CouplModelHeatWaterTransprtGenericHLWRepSalt_1.pdf.

(22) Bérest, P.; Ghoreychi, M.; Hadj-Hassen, F.; Tijani, M., Eds. *Mechanical Behaviour of Salt VII*; CRC Press: London, 2012.

(23) Olivella, S.; Gens, A. A Constitutive Model for Crushed Salt. *Int. J. Numer. Anal. Meth. Geomech.* **2002**, *26*, 719−746.

(24) Blanco Martín, L.; Wolters, R.; Rutqvist, J.; Lux, K.-H.; Birkholzer, J. T. Comparison of two simulators to investigate thermal−hydraulic−mechanical processes related to nuclear waste isolation in saliferous formations. *Comput. Geotechnics* **2015**, *66*, 219−229 DOI: 10.1016/j.compgeo.2015.01.021.

(25) Clayton, D. J.; Gable, C. W. *3-D Thermal Analyses of High Level Waste Emplaced in a Generic Salt Repository*; Sandia National Laboratories Report, SAND2009-0633P; 2009.

(26) Stone, C. M.; Holland, J. F.; Bean, J. E.; Arguello, J. G. Coupled thermal-mechanical analyses of a generic salt repository for high level

DOI: 10.1021/acs.est.5b01002
Environ. Sci. Technol. 2015, 49, 6783−6790

waste. In *44th U.S. Rock Mechanics Symposium and 5th U.S.-Canada Rock Mechanics Symposium*; Salt Lake City, UT, June 27−30, 2010.
(27) Urai, J. L.; Spiers, C. J.; Zwart, H. J.; Lister, G. S. Weakening of rock salt by water during long-term creep. *Nature* **1986**, *324*, 554−557.
(28) Zyvoloski, G. A.; Robinson, B. A.; Dash, Z. V.; Trease, L. L. *Summary of the Models and Methods for the FEHM Application*; Los Alamos National Laboratory Report, LA-13307-MS; 1999; https://fehm.lanl.gov/pdfs/fehm_mms.pdf.
(29) Cinar, Y.; Pusch, G.; Reitenbach, V. Petrophysical and capillary properties of compacted salt. *Transp. Porous Media* **2006**, *64* (2), 199−228 DOI: 10.1007/s11242-005-2848-1.
(30) Sparrow, B. S. Empirical equations for the thermodynamic properties of aqueous sodium chloride. *Desalination* **2003**, *159* (2), 161−170.
(31) Millington, R. J.; Quirk, J. P. Permeability of porous solids. *Trans. Faraday Soc.* **1961**, *57*, 1200−1207.
(32) Callahan, G. D.; Mellegard, K. D.; Hansen, F. D. Constitutive behavior of reconsolidating crushed salt. *Int. J. Rock Mech. Mining Sci.* **1998**, *35* (4), 422−423.
(33) Caporuscio, F. A.; Boukhalfa, H.; Cheshire, M. C.; Ding, M. *Brine Migration Experimental Studies for Salt Repositories*; Los Alamos National Laboratory Report, LA-UR-14-26603; 2014; http://permalink.lanl.gov/object/tr?what=info:lanl-repo/lareport/LA-UR-14-26603.
(34) Bradshaw, R. L.; McClain, W. C. *Project Salt Vault: A Demonstration of Disposal of High-Activity Solidified Wastes in Underground Salt Mines*; Oak Ridge National Laboratory Document ORNL-4555; 1971.
(35) Birkholzer, J. T. Estimating liquid fluxes in thermally perturbed fractured rock using measured temperature profiles. *J. Hydrol.* **2006**, *327* (3−4), 496−515 DOI: 10.1016/j.jhydrol.2005.11.049.

DOI: 10.1021/acs.est.5b01002
Environ. Sci. Technol. 2015, 49, 6783−6790